

**OPTIMIZATION OF STIFFENED  
LAMINATED COMPOSITE CYLINDRICAL  
PANELS IN THE BUCKLING AND  
POSTBUCKLING ANALYSIS.**

*A. Korjakin, A. Ivahskov, A. Kovalev*

Stiffened plates and curved panels are widely used as primary structural elements in aerospace, marine and civil engineering. Their stable postbuckling behavior and their capability to sustain loads far in excess of their initial buckling loads may lead to considerable weight savings, if their postbuckling strength is fully utilized and possible fatigue problems are eliminated. In the presence of large deflections, bifurcations, load and displacement limit points, the analysis of arbitrary anisotropic shells requires the adoption of incremental and iterative procedures capable of tracing the complete load-displacement path. Although the true response is dynamic in nature, a fully static solution is followed in most cases.

Stiffened panels loaded in axial compression were extensively studied and employed in aeronautical structures in the thirties, forties and beyond, yielding the effective width.

In the last decades, the trend to optimize the design shear panels, and the employment of composites and higher strength metals, has led to similar required relative stiffnesses in both civil and aeronautical engineering. The civil engineers employ stiffer flanges in order to improve the postbuckling strength of the web and the aeronautical engineers decrease the relative flange cross-sectional area in order to save weight.

The nonlinear analysis of shells requires the efficient blend of finite element technology and path-following techniques. Due to the increased computational effort of the incremental and iterative solution process, it is imperative to obtain the structural response by simple, inexpensive and accurate finite elements.

In this paper the postbuckling performance of composite shells using computer code LS-DYNA is analysed.

## 1 Formulation of design problem

The main objective of design is weight saving. Therefore, the optimization problem can be formulated as minimum weight design problem under buckling and post-buckling constraints.

### 1.1 Design parameters of the panel

It has been proposed the configurations of the design panel with  $m=5$  blade stringers (see Fig. 1). The geometric dimensions of cylindrical panel with 5 blade stiffeners are fixed and mean a follows:  $l$  is length of the panel,  $R$  is radius of the panel,  $a$  is arc length of the panel,  $d$  is distance between the stringers and  $h_w$  is height of the stringer (web). Thickness of the skin  $t$  and thickness of the stringer  $t_s$  are parameters, which will be determined in design.

Symmetric laminates with the fixed ply angles  $90/\pm 45/0$  are considered for the skin and stiffener. The laminate lay-up for the skin is chosen as follows

$$[90_{n_1} / + 45_{n_2} / - 45_{n_2} / 0_{n_3}]_s \quad (1)$$

Here  $2*n_1$  is a total number of plies for skin in circumferential ( $90^\circ$ ) direction,  $4*n_2$  is a total number of plies in the  $\pm 45^\circ$  direction and  $2*n_3$  is total number of plies in axial ( $0^\circ$ ) direction. The ply thickness is  $tp$ . In the present calculations elastic constants are taken for UD layer from the carbon/epoxy composite material

The total thickness of plies for the half of symmetric stack of layers of skin in  $0^\circ$  direction is denoted by  $t_3$ , in  $+45^\circ$  direction by  $t_2$ , in  $-45^\circ$  direction the thickness is also  $t_2$ , and in  $90^\circ$  direction by  $t_1$ . Note that total thickness of the skin is given by

$$t = 2(t_1 + 2t_2 + t_3) \quad (2)$$

The laminate lay-up for the stringer is chosen as follows

$$[(45 / - 45)_3 / 0_{n_4}]_s \quad (3)$$

Here  $2*n_4$  is a total number of plies for the blade stringer in axial direction. The total thickness of plies for the half of symmetric stack of layers of stringer in  $0^\circ$  direction is denoted by  $t_4$ . The  $\pm 45^\circ$  direction of plies in the blade is considered in order to form connection (flange) with the skin.

The total thickness of the plies for the blade (web or rib) in  $\pm 45^\circ$  direction (for both symmetric parts of stack of layers) is fixed as  $t_5=12*tp$ . The flange thickness is fixed as  $t_6=6*tp$ .

Now we can define the vector of optimization parameters

$$\mathbf{x} = [t_1, t_2, t_3, t_4] = [x_1, x_2, x_3, x_4] \quad (4)$$

The weight of cylindrical panel ( $m=5$  for the panel with 5 blades) is as follows

$$G(\mathbf{x}) = \rho l [2a(x_1 + 2x_2 + x_3) + 2m_1 f t_6 + m_1 h_w (2x_4 + t_5)] \quad (5)$$

In optimization problem the design parameters  $\mathbf{x}$  are continuous variables, but ply number is an integer. When optimal solution is obtained the total ply thickness  $t_i$  is divided by the single ply thickness  $tp$  to calculate the number of plies for the half of symmetric stack of layers. The number of plies is rounded-off to the closest integer.

Though almost any problem in structural mechanics can be considered in principle as a transient process, it is often much simpler to ignore all transient effects and stick only with statics. The buckling and post-buckling problems may be considered as a quasi-static problem. It means the implicit analysis may be used for solving the problem. Using implicit analysis a few problems should be resolved. First of all it should be a non-linear analysis taking into account large displacements. The arc-method must be used for solving the post-buckling process. These problems may be successfully solved by using the code LS-DYNA [1].

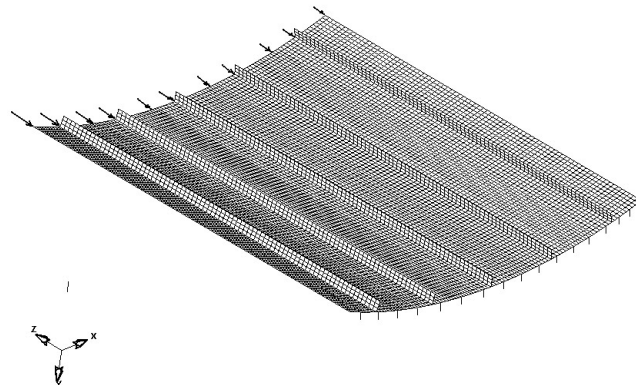


**Fig. 1. Loading of the cylindrical panel with 5 blade stiffeners.**

Dealing with a multilayered shell made from laminated composite material it is not possible to use the implicit analysis for solving the problem with LS-DYNA. So, the explicit analysis should be employed since the problem considered is a highly non-linear and deals with multilayered composite material. At the first stage of analysis particular focus was made on the sensitivity of the results concerning solution time versus loading velocity and mesh refinement. Solution time is a very important parameter due to large amount of calculations. Note that there are at least 50 variants of analysis in order to perform optimization of the geometric parameters.

A four-node shell finite element has been used for the finite element analysis. Two kind of mesh has been considered for the convergence studies. The buckling force has been used as evaluation parameter of convergence. The different between results which have been obtained using

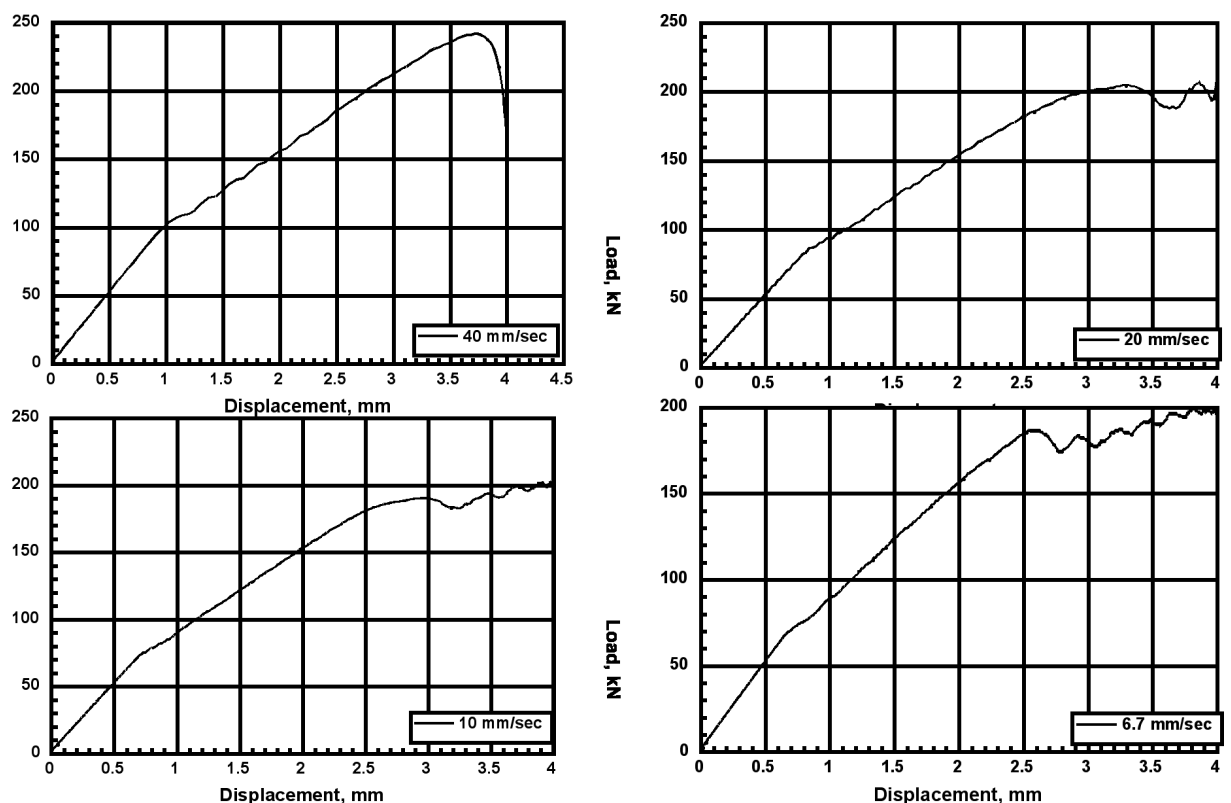


**Fig. 2. Convergence study with different load velocity.**

the mesh1 (8100 Finite elements) and mesh2 (10 000 finite elements) was 4.7%. Therefore, more fine mesh2 has been chosen for optimization calculations.

For study of the post-buckling process the displacement has been applied to the upper part of shell (see Fig 1). A comparative analysis has been implemented for the loading rate 40 mm/sec, 20 mm/sec, 10 mm/sec and 6.7 mm/sec. In Fig. 2 it is seen that the result for loading rate 10 mm/sec is better from point of view of accuracy, convergence and computational time.

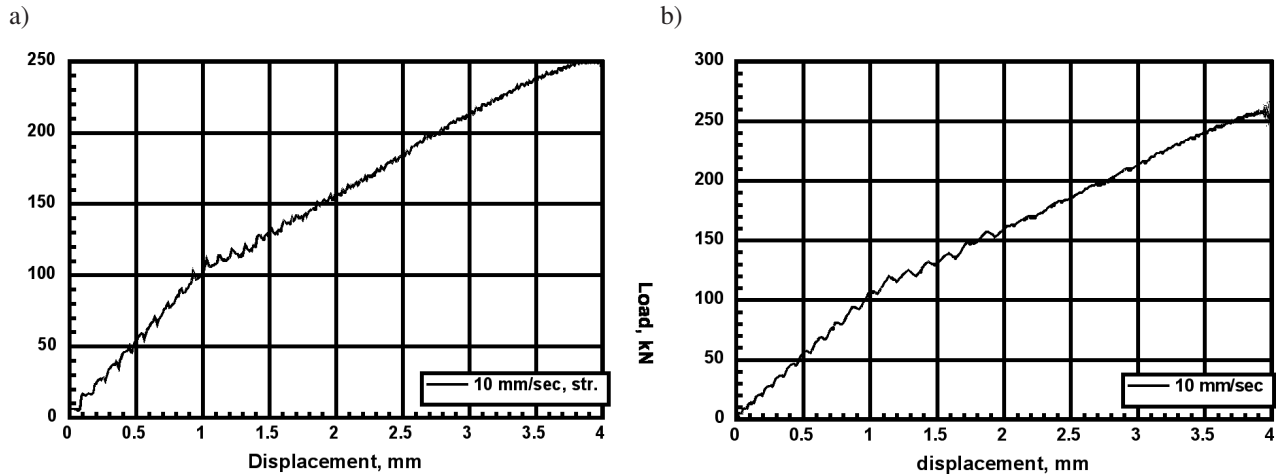


**Fig. 3. Oscillations in solution calculating with actual density.**

Employing the actual material density in the analysis considerable oscillations in the load-displacement curve can be observed, see Fig. 3a. The oscillations can be reduced using a sinusoidal form of the load-time curve. Results are shown in Fig. 3b. At the same time the problem can be considered as quasi-static. In this case 65 times reduced density is employed to avoid the oscillations, though such a method considerably increases the calculation time since with reduced density the time step should be very small.

### 1.2 Approximation of load-shortening curves

To analyze the postbuckling behavior of the shell a dynamic solution procedure is used with time integration, which is computationally very time consuming. A typical load-shortening curves are shown in Fig. 4. Results for the panel with three different layer thicknesses in the skin and blade are presented (the points of experiment design 1, 19 and 33, see below)

- 1 –  $\mathbf{x}=[0.1276, 0.1939, 0.2449, 0.7219]$ ;
- 2 –  $\mathbf{x}=[0.0357, 0.1862, 0.1633, 0.2857]$ ;
- 3 –  $\mathbf{x}=[0.1429, 0.2321, 0.2194, 0.2168]$ ;

Analyzing the curves in Fig. 4 it can be seen that all load-shortening curves for the purpose of optimization can be approximated by two lines. Such typical approximation for the panel with layer thicknesses  $\mathbf{x}=[0.125, 0.125, 0.125, 1.25]$  is shown in Fig. 5. Note that such layer thicknesses were obtained optimizing (minimum weight) the panel for the linearized (first) buckling load.

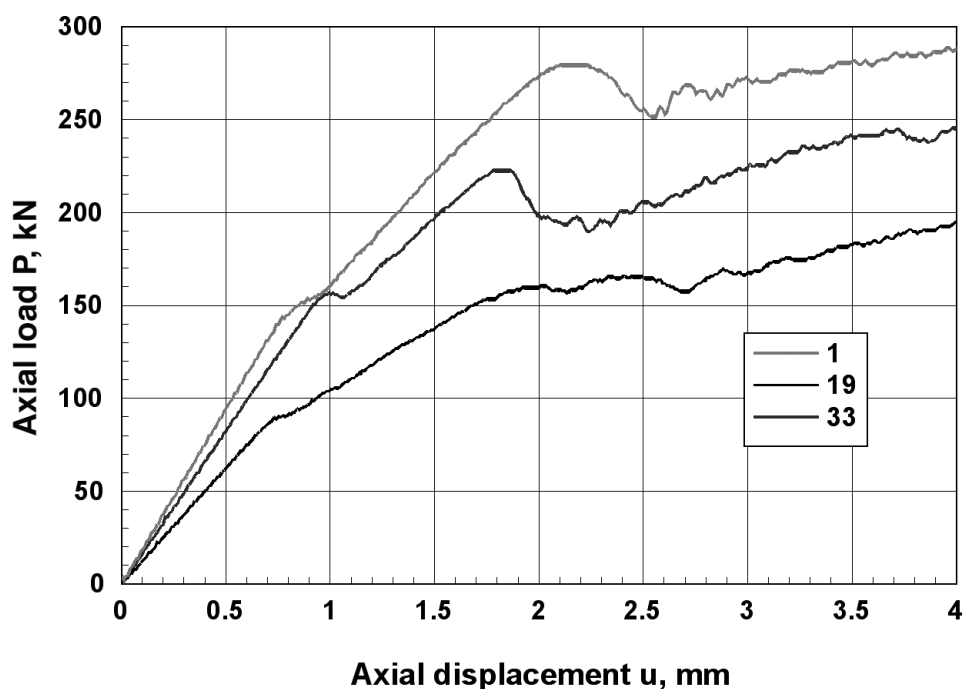


**Fig. 4. A typical load-shortening curves.**

From approximation of the pre-buckling stage (see Fig. 5) the linear axial stiffness is obtained  $k_1=119.4$  kN/mm. From approximation of the post-buckling stage the tangential axial stiffness is obtained  $k_2=79.8$  kN/mm. From the non-linear solution can be determined the first buckling load  $P_1=90.5$  kN (this is a local skin buckling mode) and the second buckling load  $P_2=225$  kN (the global buckling mode), which can be assumed as collapse load. It should be noted that the ultimate load due to failure and damage or delaminations of the material could be lower than collapse load. The failure of material depends on stresses in the post-buckling stage. Here the failure of material is not calculated and only the collapse load due to buckling is considered.

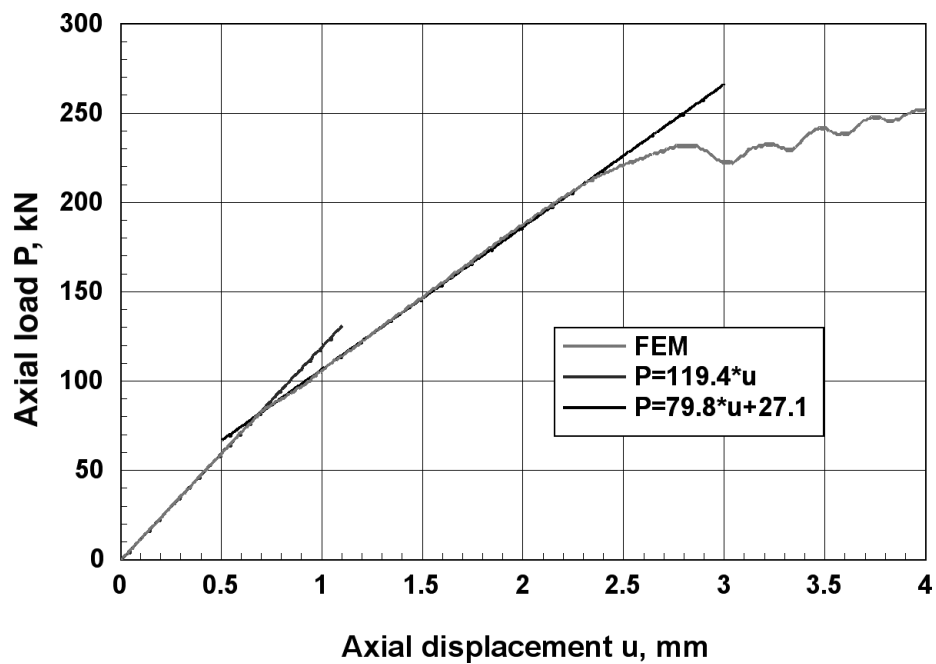


**Fig. 5. Approximation of load-shortening curve.**

### 1.3 Formulation of optimization problem for post-buckling

In the present formulation the optimization for post-buckling is considered. The post-buckling behavior of the panel is schematically represented in Fig. 6. In Fig. 6  $u$  is axial displacement, the ultimate or collapse load is denoted as  $P_2(x)$ , the linear axial stiffness of the panel in the pre-buckling state is  $k_1 = \text{tg}\alpha_0$ , the tangential (post-buckling) axial stiffness is  $k_2 = \text{tg}\alpha$ .

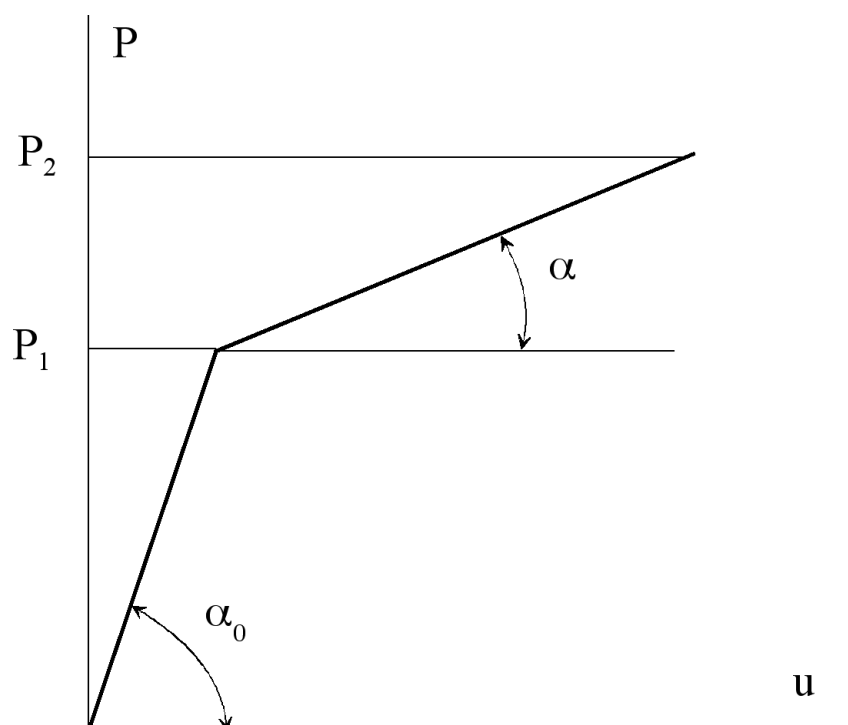


**Fig. 6. The load-shortening curve of the panel.**

The optimization problem for the second formulation is as follows. Minimize the weight of panel

$$G(\mathbf{x}) \rightarrow \min \quad (6)$$

subject to buckling and axial stiffness constraints

$$P_1(\mathbf{x}) \geq P_1^* \quad (7)$$

$$P_2(\mathbf{x}) \geq P_2^* \quad (8)$$

$$k_1(\mathbf{x}) \geq k_1^* \quad (9)$$

$$k_2(\mathbf{x}) \geq k_2^* \quad (10)$$

and lower and upper bound constraints for parameters

$$x_i^{\min} \leq x_i \leq x_i^{\max}, i=1,2,3,4 \quad (11)$$

Here  $P1^*$ ,  $P2^*$ ,  $k1^*$ ,  $k2^*$  are the limits of loads and axial stiffnesses selected by the designer. For example, for mild axial stiffness reduction in the post-buckling stage in comparison with the pre-buckling stage the value  $k2^*$  could be about 30% lower than  $k1^*$ . For strong axial stiffness reduction in the post-buckling stage  $k2^*$  could be more than 50% lower than  $k1^*$ . The load limits  $P1^*$ ,  $P2^*$  can be chosen under considerations of limiting the local and global buckling loads. The constraints (11) define the domain of interest. In this domain the experiment design is performed (see below).

## 2 Solution of the optimization problem

Solution of the optimization problem can be obtained using the finite element method, the method of experiment design and the response surface approach [2-4].

### 2.1 Design of experiments

Optimum design of the panel (see Fig. 1) using the formulation with post-buckling constraints is performed using a plan of experiment with 50 reference points. The lower  $x_j^{\min}$  and the upper  $x_j^{\max}$  bounds (domain of interest) for the optimization parameters are chosen as follows

$$\begin{aligned} 0 &\leq x_1 \leq 0.250 \\ 0.125 &\leq x_2 \leq 0.5 \\ 0 &\leq x_3 \leq 0.250 \\ 0.125 &\leq x_4 \leq 1.25 \end{aligned} \quad (12)$$

So, for the half of symmetric stack of layers in corresponding directions (0, +45, -45, 90) there could be from two to twelve plies. Thus, for the constraints (12) a minimum total thickness of skin could be 0.25 mm (2 plies), the minimum total thickness of rib could be 1.75 mm. A maximum total thickness of the skin could be 3 mm (24 plies), the maximum total thickness of the rib could be 4 mm.

The values of optimization parameters  $x_i$  in the reference points of the domain of interest are calculated by the formula

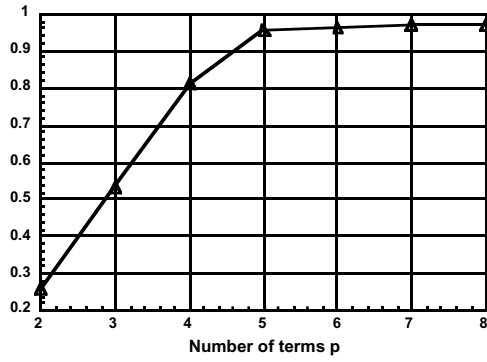
$$x_j^{(i)} = x_j^{\min} + \frac{1}{k-1}(x_j^{\max} - x_j^{\min})(B_{ij} - 1) \quad (13)$$

Here  $i=1,2,\dots,k$  and  $j=1,2,\dots,n$ , where in our case the number of experiments  $k=50$  and the number of variables  $n=4$ . Corresponding matrix of experiment design  $B_{ij}$  was calculated using the program PLANI. In all these 50 reference points the non-linear buckling analysis was performed. The load-shortening curves for three points of experiment design (points 1, 19, 33) are shown in Fig. 4. Computational time for solution of the non-linear buckling problem for one point of experiment design is about 10 to 16 hours on Workstation IBM RS/6000, 44P, Model 170, 1 Gb RAM or 24 to 38 hours on PC Pentium III, 600 MHz.

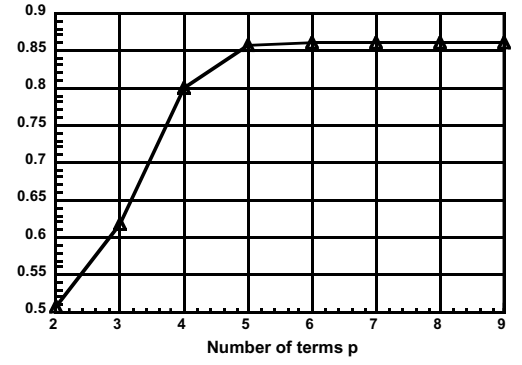
Employing the load-shortening curves the linear approximations for pre- and post-buckling stages are performed and the values of axial stiffnesses  $k_1$  and  $k_2$  are obtained. Also the values of the first buckling load  $P_1$  and the collapse load  $P_2$  are determined.

### 2.2 Approximating functions

Having information about values of all four functions in all 50 points of experiment design the approximating functions (model functions) for the axial stiffnesses  $k_1$  and  $k_2$  as well as for the first buckling load  $P_1$  and the collapse load  $P_2$  can be determined. For this the software code RESINT is used and the approximating function is built. The main 'trick' of the present approach for building a model function is a step by step term reduction in the approximating function (see Figs. 7 and 8). The 'best' model corresponds to the break in the term reduction diagram. For all functions the first break in the diagram is seen definitely.



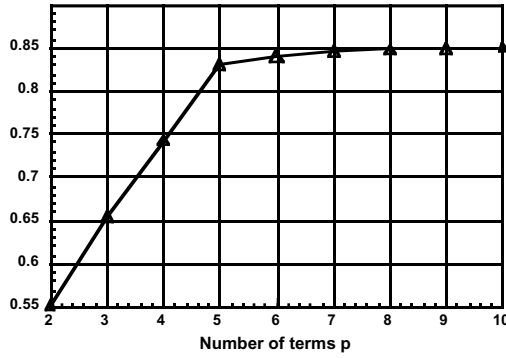
a)



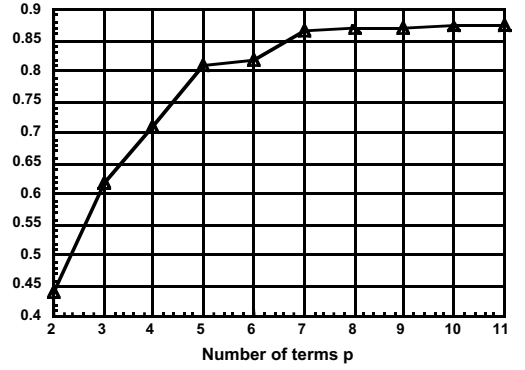
b)

**Fig. 7.**

**a) Diagram of term reduction for the function  $k_1$ , b) Diagram of term reduction for the function  $k_2$**



a)



b)

**Fig. 8.**

**a) Diagram of term reduction for the function  $P_1$ , b) Diagram of term reduction for the function  $P_2$**

Thus, for the function  $k_1$  the break in the diagram (see Fig. 7a) is for  $p=5$ , which corresponds to model function with 5 terms (correlation  $c=0.955$ )

$$k_1(\mathbf{x}) = -7.143 + 285.2x_2 + 352.7x_3 + 53.37x_4 + 104.9x_1 \quad (14)$$

It is seen that pre-buckling axial stiffness is a simple linear function of design parameters. Expected precision of this function in the domain of interest is about 5%. This means that difference between the value of original function obtained by FEM solution and the model function (14) in any other point of domain of interest will not exceed 4.45% (or the expected deviation will not exceed 0.445 from the range of function in the domain).

For the function  $k_2$  the break in the diagram (see Fig. 7b) is also for  $p=5$ , which corresponds to model function with 5 terms (correlation  $c=0.858$ )

$$k_2(\mathbf{x}) = -30.60 + 326.9x_2 + 49.11x_4 + 93.40x_1 + 711.5x_2x_3 \quad (15)$$

Expected precision of this function is lower – only about 15%.

For the function  $P_1$  the break in the diagram (see Fig. 8a) is again for  $p=5$ , which corresponds to model function with 5 terms (correlation  $c=0.831$ )

$$P_1(\mathbf{x}) = -30.02 + 397.9x_2 + 1137x_1x_2 + 756.9x_2x_3 + 211.3x_2x_4 \quad (16)$$

Expected precision of this function is about 17%.

For the function  $P_2$  the break in the diagram (see Fig. 8b) is also for  $p=7$ , which corresponds to model function with 7 terms (correlation  $c=0.865$ )

$$P_2(\mathbf{x}) = -119.9 + 860.4x_2 + 152.0x_4 + 336.7x_1 + 958.8x_3 - 3633x_2x_3 + 13740x_2^3x_3 \quad (17)$$

Expected precision of this function is about 13%.

It should be emphasized that the model functions (14)-(17) can be used for the panel (Fig. 1) with 5 ribs and only in the selected domain (12) since approximating function is built for this domain. Now for the optimum design the simple model functions (14)-(17) can be used in the buckling and stiffness constraints (7)-(10) instead of original functions numerically calculated by FEM.

### 2.3 Results of optimization

The optimization problem is solved employing a conventional method of non-linear programming – a Sequential Quadratic Programming (SQP) method. For this the MATLAB software is used [5].

Two designs are considered for the given loads and stiffnesses in constraints (7)-(10)

$$1) P_I^*=130 \text{ kN}; k_I^*=100 \text{ kN/mm}; k_2^*=50 \text{ kN/mm}; P_2^*=300 \text{ kN};$$

$$2) P_I^*=100 \text{ kN}; k_I^*=100 \text{ kN/mm}; k_2^*=50 \text{ kN/mm}; P_2^*=300 \text{ kN};$$

Results of optimization for design 1 are as follows

$$\mathbf{x}^*=[0.0532, 0.1961, 0.1236, 1.25]; G^*=1.486 \text{ kg};$$

Here  $\mathbf{x}^*$  is vector of design parameters for optimum (minimum weight) and  $\mathbf{x}^{**}$  is vector of rounded-off design parameters for optimum

$$\mathbf{x}^{**}=[0, 0.25, 0.125, 1.25]; G^{**}=1.562 \text{ kg}; \quad (18)$$

In the point of optimum active are constraints for the first buckling load (7) and for the collapse load (8). Constraints for stiffnesses (9)-(10) are not active and values of constraint functions are as follows

$$P_I(\mathbf{x}^*)=130 \text{ kN}; P_2(\mathbf{x}^*)=300 \text{ kN}; k_I(\mathbf{x}^*)=164 \text{ kN/mm}; k_2(\mathbf{x}^*)=117 \text{ kN/mm};$$

Calculated constraint functions for rounded-off values of parameters  $\mathbf{x}^{**}$  are given by

$$P_I(\mathbf{x}^{**})=159 \text{ kN}; P_2(\mathbf{x}^{**})=318 \text{ kN}; k_I(\mathbf{x}^{**})=175 \text{ kN/mm}; k_2(\mathbf{x}^{**})=135 \text{ kN/mm}; \quad (19)$$

Results of optimization for design 2 are as follows

$$\mathbf{x}^*=[0, 0.2672, 0, 1.25]; G^*=1.438 \text{ kg}; \quad (20)$$

Only the constraint for the collapse load (8) is active

$$P_I(\mathbf{x}^*)=146 \text{ kN}; P_2(\mathbf{x}^*)=300 \text{ kN}; k_I(\mathbf{x}^*)=135 \text{ kN/mm}; k_2(\mathbf{x}^*)=118 \text{ kN/mm};$$

The rounded-off values of parameters are given by

$$\mathbf{x}^{**}=[0, 0.25, 0, 1.25]; G^{**}=1.391 \text{ kg}; \quad (21)$$

Calculated constraint functions for rounded-off values of parameters  $\mathbf{x}^{**}$  are given by

$$P_I(\mathbf{x}^{**})=135 \text{ kN}; P_2(\mathbf{x}^{**})=285 \text{ kN}; k_I(\mathbf{x}^{**})=131 \text{ kN/mm}; k_2(\mathbf{x}^{**})=113 \text{ kN/mm}; \quad (22)$$

The first optimum solution (20) was obtained from the starting point

$$\mathbf{x}=[0.5, 0.5, 0.5, 0.5];$$

The second solution of design 2 was obtained from the starting point

$$\mathbf{x}=[0.1, 0.1, 0.1, 0.1];$$

The second optimum solution for this non convex problem is as follows

$$\mathbf{x}^*=[0, 0.1578, 0.2142, 1.25]; G^*=1.432 \text{ kg}; \quad (23)$$

It is seen that for both solutions (20) and (23) the value of cost function (weight) is about the same, but parameters are different. For the second solution the constraints for the first buckling load (7) and for the collapse load (8) are active

$$P_I(\mathbf{x}^*)=100 \text{ kN}; P_2(\mathbf{x}^*)=300 \text{ kN}; k_I(\mathbf{x}^*)=180 \text{ kN/mm}; k_2(\mathbf{x}^*)=106 \text{ kN/mm};$$

For the second solution the rounded-off values of parameters are given by

$$\mathbf{x}^{**}=[0, 0.125, 0.25, 1.25]; G^{**}=1.391 \text{ kg}; \quad (24)$$

It is seen that for both solutions (21) and (24) the value of cost function is the same, however, the skin laminates are different.

Calculated constraint functions for rounded-off values of parameters  $\mathbf{x}^{**}$  for the second solution are given by

$$P_I(\mathbf{x}^{**})=76 \text{ kN}; P_2(\mathbf{x}^{**})=310 \text{ kN}; k_I(\mathbf{x}^{**})=183 \text{ kN/mm}; k_2(\mathbf{x}^{**})=94 \text{ kN/mm}; \quad (25)$$

Note that for both solutions (for rounded-off values) the buckling constraints are violated. In the first solution the constraint (8) for collapse load is violated for 5%. In the second solution the constraint (7) for the first buckling load is violated for 24%. So, as satisfactory design the first solution (21) can be chosen.

### 2.4 Verification of optimum solution by FEM

Verification by FE analysis is performed for the first variant (18) of design. The calculated values (19) of constraint functions (14)-(17) are also employed to build the surrogate model (SM) of the load-shortening curve. In Fig. 9 the load-shortening curve obtained by FEM (LS-DYNA) for the design (18) is presented.

Employing the values (19), which are calculated values of approximating functions (14)-(17) in the point of design  $\mathbf{x}^{**}=[0, 0.25, 0.125, 1.25]$ , the surrogate model of the load-shortening curve of the present design can be built

$$P_I(u) = k_1 u; P_{II} = k_2 u + P_1 \left(1 - \frac{k_2}{k_1}\right); P_{III} = P_2 \quad (26)$$

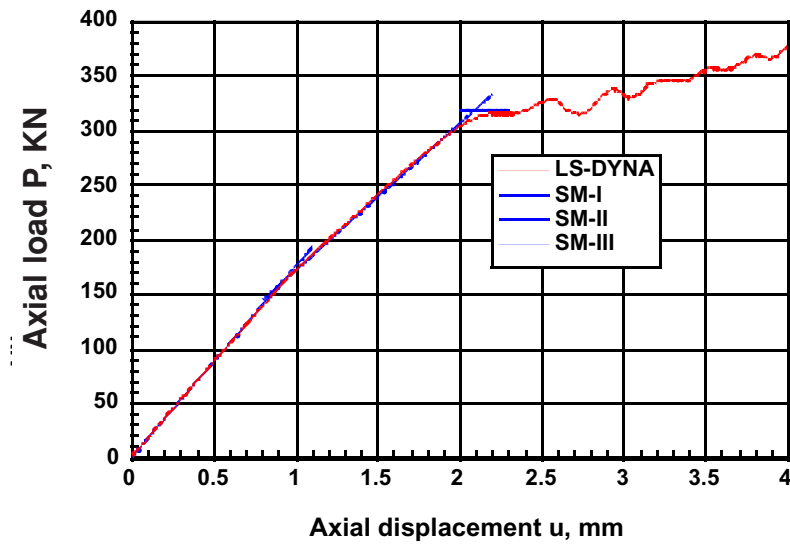


**Fig. 9. Load-shortening curve obtained by FEM and surrogate models for the first variant of design (19) -  $x^{**}=[0, 0.25, 0.125, 1.25]$**

Here for design (18) the values are as follows

$$P_1=159 \text{ kN}; P_2=318 \text{ kN}; k_1=175 \text{ kN/mm}; k_2=135 \text{ kN/mm}; \quad (27)$$

The surrogate model of the load-shortening curve represented by three lines (SM-I, SM-II, SM-III) is shown in Fig. 9. It is seen good agreement with the curve calculated by FEM. Note that these three lines are not approximation of the FEM solution, but built based on functions (14)-(17). For comparison by approximation of the load-shortening curve in Fig. 9 obtained by FEM the following values of pre- and post-buckling stiffnesses were obtained

$$k_1=173 \text{ kN/mm}; k_2=134.2 \text{ kN/mm}; \quad (28)$$

STEP 220 TIME = 2.1899666E-01

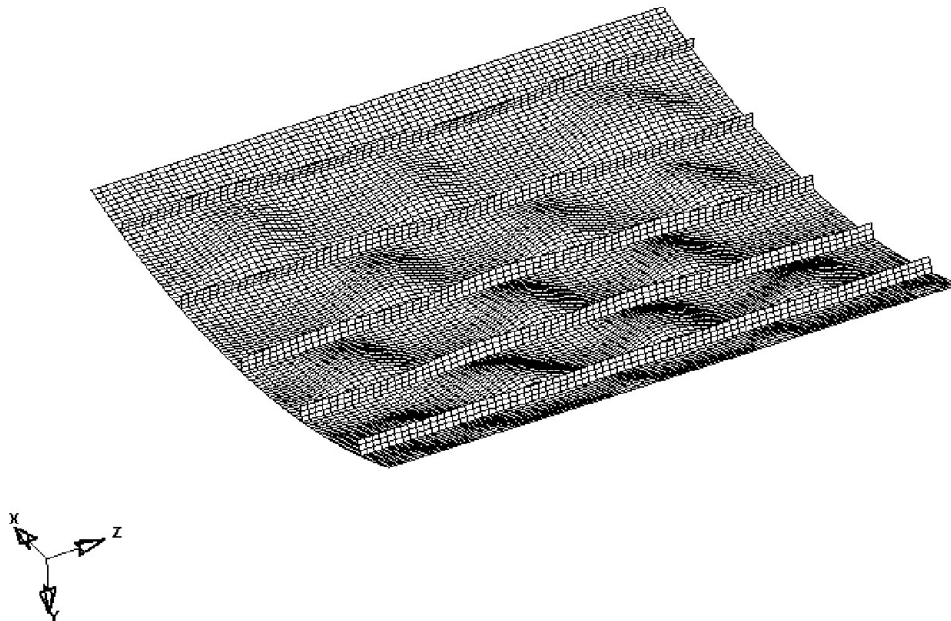


**Fig. 10. Buckling mode corresponding to the collapse load  $P_2=318 \text{ kN}$  for the first variant of design (18) with  $x^{**}=[0, 0.25, 0.125, 1.25]$  – inside view.**

These values are close to the values (27) obtained from the approximating functions (14) and (15).

Thus, substituting the approximating functions (14)-(17) in the surrogate model of load-shortening curve (26) for different designs  $x$  the pre- and post-buckling shortening curve can be easily calculated.

Of course, the buckling modes can be obtained only by FE analysis. In Fig. 10 the mode corresponding to the collapse load  $P_2=318 \text{ kN}$  for the first variant of design (18) with  $x^{**}=[0, 0.25, 0.125, 1.25]$  is presented.

## Conclusions

The applicability of explicit program LS-DYNA to quasi-static analysis of the shell postbuckling behavior was shown. The method of experiment design can be used for the weight optimization for post-buckling. Computational time for one reference point is from 10 to 16 hours on powerful workstation. At all at least 50 reference points should be calculated to obtain the approximating functions for the first buckling load, for the collapse load, for the pre- and post-buckling axial stiffness. These approximating functions are used for optimization purposes. Employing the approximating functions the surrogate model for the load-shortening curve is obtained. This surrogate model can be used for the fast reanalysis in the post-buckling stage.

## *References*

1. LS-DYNA. Ver. 950D. Theoretical manual. Livermore Software Technology Corporation, 1998.
2. Rikards, R., Chate, A., Optimal Design of Sandwich and Laminated Composite Plates Based on Planning of Experiments, *Structural Optimization*, 10, (1), 1995, 46-53.
3. Rikards, R. and Chate A., Identification of elastic properties of composites by method of planning of experiments, *Composite Structures*, 42 (3), 1998, 257-263.
4. Rikards, R., Chate, A., Steinchen, W., Kessler, A. and Bledzki, A. K. Method for identification of elastic properties of laminates based on experiment design, *Composites. Part B*, 30, 1999, 279-289.
5. MATLAB. Version 5.1. Optimization Toolbox User's Guide, The MathWorks Inc., Natick, Mass., USA, 1997.